High order edge finite element approximations for the time-harmonic Maxwell's equations

Conference Paper · January 2015

DOI: 10.1109/CAMA.2014.7003328

CITATIONS
3

READS
27

4 authors:

Marcella Bonazzoli
National Institute for Research in Computer Science and Control
17 PUBLICATIONS **42** CITATIONS
SEE PROFILE

Elena Gaburro
Università degli Studi di Trento
8 PUBLICATIONS **7** CITATIONS
SEE PROFILE

Victorita Dolean
University of Strathclyde
105 PUBLICATIONS **1,028** CITATIONS
SEE PROFILE

Francesca Rapetti
University of Nice Sophia Antipolis
95 PUBLICATIONS **990** CITATIONS
SEE PROFILE

High order edge finite element approximations for the time-harmonic Maxwell's equations

Marcella Bonazzoli*, Elena Gaburro*,Victorita Dolean†, Francesca Rapetti*
*Laboratoire J.-A. Dieudonné
Université de Nice-Sophia Antipolis, Parc Valrose, 06108 Nice Cedex 02
Email: marcella@bonazzoli.it, elenagaburro@gmail.com, Francesca.Rapetti@unice.fr
†Department of Mathematics and Statistics, University of Strathclyde, Glasgow G1 1XH
Email: Victorita.Dolean@strath.ac.uk

***Abstract*—The time-harmonic Maxwell equations model the propagation of electromagnetic waves and are therefore fundamental equations for the simulation of many modern devices in everyday life. The numerical solution of these equations is hampered by some fundamental problems especially in high frequency regime. Fine meshes have to be used in order to represent well the solution and also to avoid the pollution effect, which is very well known for the Helmholtz equations. We propose in this paper to address this problem by considering high order finite element approximations and in particular Whitney edge elements.**

I. Introduction

Low order edge elements are widely used for electromagnetic field problems, and high order edge approximation are receiving increasing interest but their definition become rather complex. Most of the existing constructions of high order extensions of Whitney edge elements follow the traditional FEM path of using higher and higher moments to define the needed degrees of freedom (dofs). As a result, such high order finite elements include non-physical dofs (like face or volume moments) that are not easy to interpret as field circulations along edges (which are the dofs in the low degree case). We propose here a high order implementation which remove this inconvenient feature and apply it to the case of the Maxwell's equations in frequency regime.

The second order formulation of the time-harmonic Maxwell equations is given by

$$(-\omega^2\varepsilon + i\omega\sigma)\mathbf{E} + \nabla \times \left(\frac{1}{\mu}\nabla \times \mathbf{E}\right) = -i\omega\mathbf{J}. \qquad (1)$$

where $\mathbf{E}$ is the complex amplitude of the electromagnetic field supposing a periodic behaviour in time given by the frequency ω, ε is the electric permittivity, μ the magnetic permeability and σ the conductivity of the medium. Here $\mathbf{J}$ denotes the amplitude of the imposed source of current. Consider the domain $\Omega = [0, c] \times [0, b]$ which could be a two-dimensional waveguide and the outward normal is denoted by $\mathbf{n}$. We will concentrate on the spatial discretization of the following boundary value problem

$$\begin{cases} \kappa\mathbf{E} + \nabla \times \left(\frac{1}{\mu}\nabla \times \mathbf{E}\right) = 0, & \text{in } \Omega, \\ \mathbf{E} \times \mathbf{n} = 0, & \text{on } \Gamma_m, \\ \nabla \times \mathbf{E} \times \mathbf{n} + i\beta\mathbf{n} \times (\mathbf{E} \times \mathbf{n}) = g^{inc}, & \text{on } \Gamma_{inc}, \\ \nabla \times \mathbf{E} \times \mathbf{n} + i\beta\mathbf{n} \times (\mathbf{E} \times \mathbf{n}) = 0, & \text{on } \Gamma_{out}. \end{cases} \qquad (2)$$

where $\kappa = i\omega\sigma - \omega^2\varepsilon$, $g^{inc} = 2i\beta\mathbf{E}^{inc}$, $\Gamma_m = \{\mathbf{x} \in \partial\Omega, x = 0, \text{or } x = a\}$ is the metallic part of the boundary, $\Gamma_{inc} = \{\mathbf{x} \in \partial\Omega, y = 0\}$, $\Gamma_{out} = \{\mathbf{x} \in \partial\Omega, y = b\}$, β is the impedance parameter and $\mathbf{E}^{inc}$ denotes the incident field or excitation imposed at the incoming part of the boundary Γ_{inc}.

The week formulation is obtained by multiplying (2) by a test function $\mathbf{v}$ and integrating by parts. On Γ^m we choose the test function $\mathbf{v} \in H(\text{curl}, \Omega)$ (where $H(\text{curl}, \Omega)$ is the space of square integrable functions whose curl is also square integrable), such that $\mathbf{v} \times \mathbf{n} = 0$ and on the other boundaries we simply replace the impedance boundary conditions

$$\int_\Omega \kappa\mathbf{E} \cdot \mathbf{v} + \left(\tfrac{1}{\mu}\nabla \times \mathbf{E}\right) \cdot (\nabla \times \mathbf{v})\, dx + \int_{\Gamma^{inc} \cup \Gamma^{out}} \tfrac{i\beta}{\mu} (\mathbf{E} \times \mathbf{n}) \cdot (\mathbf{v} \times \mathbf{n})\, d\sigma = \int_{\Gamma^{inc}} \tfrac{1}{\mu} g^{inc} \cdot \mathbf{v} d\sigma. \qquad (3)$$

We want to find an approximation of the continuous variational problem (3). In order to do this we look for a finite dimensional space $V_h \subset H(\text{curl}, \Omega)$. Suppose that $\Omega \subset \mathbb{R}^2$ can be covered by a triangulation $\mathcal{T}_h$ where the intersection of two elements of $\mathcal{T}_h$ whether is empty, one edge or the whole element. The simplest possible conformal discretization is given by the low order Nédélec finite elements [1]. The local basis functions for V_h are associated to the edges E from the vertex l to the vertex m of a given triangle t of $\mathcal{T}_h$ and they are given by

$$w^E = \lambda_l \nabla\lambda_m - \lambda_l \nabla\lambda_m.$$

where the λ_l are the barycentric coordinates.

II. High order finite element approximation

We follow here the approach presented in [2]. The strategy of building the basis functions is rather simple. Inside each triangle of the mesh (which will be called *big triangle*) we consider an increasing number of *small triangles* homothetic to the big one, associated with the principal lattice of the big triangle (see figure 1). The degrees of freedom (and the

corresponding basis functions) are associated with each *small edge* of each small triangle, and they have a rather easy *physical* interpretation: the circulation of the field along an edge can be found as a linear combination of these degrees of freedom. The orientation given by the mesh for each triangle is counterclockwise, but in this way, for two adjacent triangles, the induced orientation of the common edge is different according to the triangle from which it is seen. So we have to choose a unique global orientation for the basis functions associated to the degrees of freedom of the unknowns vector: each edge is oriented from the vertex with the smallest global number to the vertex with the biggest one. If we denote by $\lambda^{\mathbf{k}}$ the monomial $\lambda_1^{k_1}\lambda_2^{k_2}\lambda_3^{k_3}$, the *basis functions* of polynomial degree $k+1$ (order k) over the triangle t are

$$w^e = \lambda^{\mathbf{k}} w^E,$$

for all big edges E of the triangle t, and for all multi-indices $\mathbf{k}$ with 3 components and of weight k. Hence in dimension 2 we have $3 \cdot \binom{k+2}{2}$ basis functions for each big triangle.

The basis function w^e is associated with the *small edge* $e = \{\mathbf{k}, E\}$ which can be found, given E and $\mathbf{k}$, as the image of E through the function $\tilde{\mathbf{k}}$. The $\tilde{\mathbf{k}}$ map, corresponding to the multi-index $\mathbf{k}$, is the homothety which maps a point $x \in t$ onto the point of t with barycentric coordinates $\tilde{k}_i(\lambda_i(x)) = \frac{\lambda_i(x)+k_i}{k+1}$. We remark that the image $\tilde{\mathbf{k}}(t)$ of the triangle t is a small triangle homothetic to t (see the blue triangles in figure 1 and see figure 2 for the action of the $\tilde{\mathbf{k}}$ map).

Therefore, given a multi-index $\mathbf{k}$, we can build 3 basis functions which are associated to the small edges $e = \{\mathbf{k}, E\}$ of the same small triangle; in practice, to find the small edge e we can think that E says that e is parallel to the big edge E, and that each component of $\mathbf{k}$ says how near the small triangle is to each vertex of the big triangle (higher is k_i nearer is the small triangle to the i-th vertex).

The orientation of the small edges $e = \{\mathbf{k}, E\}$, and so the one of the corresponding basis functions, is given by the orientation of the big edge E.

Despite these basis functions are very simple to generate, they are not linearly independent, indeed for each small triangle which is not homothetic to the big one (the white ones in figure 1) there is a *relation* among the basis functions associated with its small edges: the sum of these functions, each of them taken with the sign coming from the global orientation, is zero.

Since the matrix A associated with our discretized equation would be singular, we have to add the equations coming from the relations described above. So we build a rectangular sparse matrix R with (number of triangles $\times$ number of relations) rows and (number of dofs) columns, whose non-zero elements are only 1 and -1. Hence the linear system, with such constraints, becomes:

$$\begin{pmatrix} A & R^T \\ R & 0 \end{pmatrix} \begin{pmatrix} u \\ \lambda \end{pmatrix} = \begin{pmatrix} b \\ 0 \end{pmatrix},$$

where u is the vector of dofs, λ is a vector of auxiliary unknowns and b is the original right-hand side.

TABLE II
NUMBER OF DOFS FOR THE CHOSEN VALUES OF h AND k

number of dofs	$k=0$	$k=1$	$k=2$	$k=3$	$k=4$
h_1	17	58	123	212	325
h_2	33	114	243	420	645
h_3	65	226	483	836	1285
h_4	129	450	963	1668	2565
h_5	450	1668	3654	6408	9930

Another difficulty with these elements is that the small edges and the basis functions are not in duality via the circulation. As a result, imposing a Dirichlet boundary condition by the penalty method is not as easy as usual. Consider for example a vector field U, whose dofs over a triangle t are $u_1, \ldots, u_n$, and a Dirichlet data g. Since $\int_{e_i} w^{e_j} \cdot \tau \neq \delta_{ij}$, to impose the condition

$$\int_{e_i} U \cdot \tau = \int_{e_i} g \cdot \tau,$$

where τ is the tangent vector to the small edge e_i of t, a priori we have to consider all the dofs as follows

$$\int_{e_i} U \cdot \tau = \sum_j u_j \int_{e_i} w^{e_j} \cdot \tau = \int_{e_i} g \cdot \tau.$$

Hence, calling I and J the global indices corresponding to the local indices i and j, we have to set the I-th row of the matrix to zero, add in the (I, J) positions of the matrix the non-zero terms $\int_{e_i} w^{e_j} \cdot \tau$ and set the I-th entry of the right-hand side equal to $\int_{e_i} g \cdot \tau$.

III. NUMERICAL RESULTS

In order to verify that our code is correctly implemented and to compute the convergence orders, we choose as exact solution $\mathbf{E} = (0, e^{-\sqrt{\mu\kappa}x})$ and we compute the corresponding boundary conditions to be imposed.

We report the results obtained for a guide with $b = 0.00127$, $c = 0.0502$ and choosing as medium the air (so $\varepsilon = \varepsilon_0 = 8.85 \cdot 10^{-12}$ F/m, $\mu = \mu_0 = 1.26 \cdot 10^{-6}$ H/m and $\sigma = 0$ S·m).

We consider two high frequencies $\omega_1 = 95 \cdot 10^9$ Hz and $\omega_2 = 110 \cdot 10^9$ Hz, and for each frequency we take $k = 0, 1, 2, 3, 4$ and five discretization triangle diameters $h_1 = 1.2614 \cdot 10^{-2}$ m, $h_2 = 6.4022 \cdot 10^{-3}$ m, $h_3 = 3.3848 \cdot 10^{-3}$ m $h_4 = 2.0184 \cdot 10^{-3}$ and $h_5 = 1.0092 \cdot 10^{-3}$.

After solving the linear system, we reconstruct the field $\mathbf{E}$ over each triangle as linear combination of the basis functions with coefficients given by the related dofs, and we evaluate it at the barycentre of each triangle. To compute the numerical error of the real part, we take the maximum over all the triangles of the modulus of the difference between the values at the barycentres of the exact and the numerical solution.

In table I we report the numerical errors for ω_1 and ω_2 for the chosen values of h and k. Looking at the bold numbers along the diagonals we can see that to obtain an error of the same order of magnitude we can take a coarser mesh if we use higher degree elements. We notice also that with the same

TABLE I
NUMERICAL ERRORS FOR THE CHOSEN VALUES OF h AND k

ω_1	$k=0$	$k=1$	$k=2$	$k=3$	$k=4$
h_1		$6.2070 \cdot 10^{-1}$	$7.9900 \cdot 10^{-2}$	$1.7800 \cdot 10^{-2}$	$\mathbf{1.7000 \cdot 10^{-3}}$
h_2	$6.2330 \cdot 10^{-1}$	$7.2400 \cdot 10^{-2}$	$7.9000 \cdot 10^{-3}$	$\mathbf{7.7036 \cdot 10^{-4}}$	$5.0610 \cdot 10^{-5}$
h_3	$2.6600 \cdot 10^{-1}$	$1.3300 \cdot 10^{-2}$	$\mathbf{1.1000 \cdot 10^{-3}}$	$4.0392 \cdot 10^{-5}$	$2.7359 \cdot 10^{-6}$
h_4	$1.7490 \cdot 10^{-1}$	$\mathbf{4.5000 \cdot 10^{-3}}$	$2.2250 \cdot 10^{-4}$	$3.2660 \cdot 10^{-6}$	$1.5927 \cdot 10^{-7}$
h_5	$\mathbf{8.1000 \cdot 10^{-2}}$	$1.2000 \cdot 10^{-3}$	$2.7838 \cdot 10^{-5}$	$2.0437 \cdot 10^{-7}$	$4.9782 \cdot 10^{-9}$

ω_2	$k=0$	$k=1$	$k=2$	$k=3$	$k=4$
h_1		$7.1940 \cdot 10^{-1}$	$1.6720 \cdot 10^{-1}$	$3.4700 \cdot 10^{-2}$	$\mathbf{4.2000 \cdot 10^{-3}}$
h_2	$7.2750 \cdot 10^{-1}$	$1.2290 \cdot 10^{-1}$	$1.4200 \cdot 10^{-2}$	$\mathbf{1.5000 \cdot 10^{-3}}$	$1.0719 \cdot 10^{-4}$
h_3	$3.2280 \cdot 10^{-1}$	$1.8600 \cdot 10^{-2}$	$\mathbf{1.7000 \cdot 10^{-3}}$	$7.4215 \cdot 10^{-5}$	$5.7051 \cdot 10^{-6}$
h_4	$2.0720 \cdot 10^{-1}$	$\mathbf{6.1000 \cdot 10^{-3}}$	$3.4601 \cdot 10^{-4}$	$5.8596 \cdot 10^{-6}$	$3.3144 \cdot 10^{-7}$
h_5	$\mathbf{9.6100 \cdot 10^{-2}}$	$1.5000 \cdot 10^{-3}$	$4.3207 \cdot 10^{-5}$	$3.6727 \cdot 10^{-7}$	$1.0361 \cdot 10^{-8}$

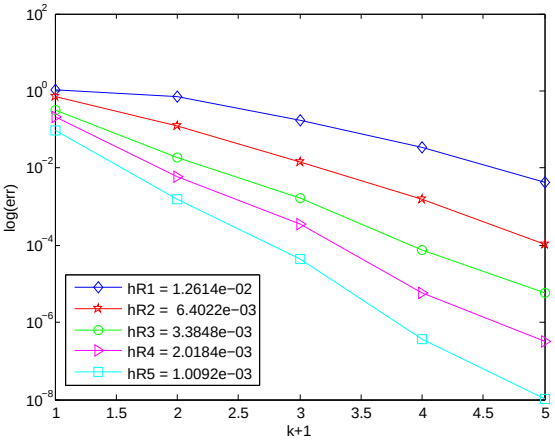

(a) k-convergence of the numerical error.

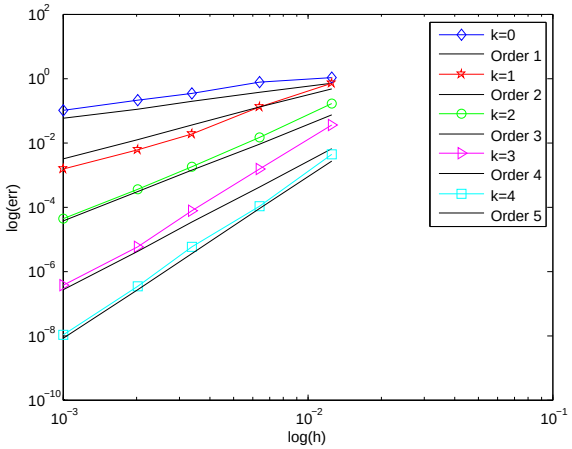

(b) h-convergence of the numerical error.

Fig. 1. Convergence orders

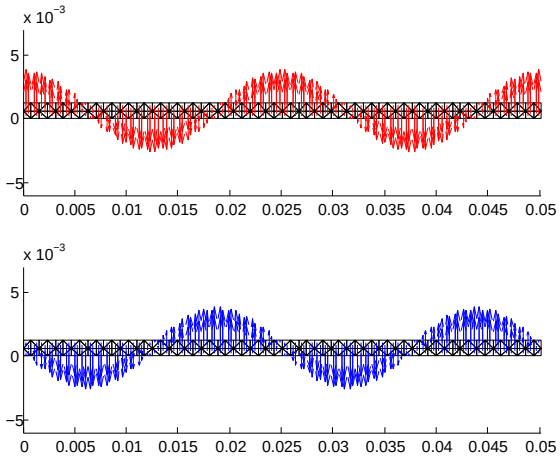

Fig. 2. Real and imaginary parts (see respectively top and bottom) of the approximated field $\mathbf{E}$ for $\sigma = 0$ S·m.

number of dofs we get a remarkably smaller error using higher order elements (see the boxed numbers in tables II and I).

Moreover, in figure 3a we show the semi-log plot of the error for the considered choices of h: a super-algebraic convergence is achieved with respect to k. We show as well in figure 3b the log-log plot of the error for the considered choices of k : the convergence to the exact solution is of algebraic type and achieved with an order of accuracy equal to $k+1$ with respect to h.

Finally we report in figure 4 the real and imaginary parts of the approximated field $\mathbf{E}$ obtained using $k=2$ and the mesh diameter h_5. If we consider the dispersion phenomenon which corresponds to non-zero conductivity ($\sigma \neq 0$), the amplitude of the field decreases from left to right (see figure 5), but the same order of accuracy is achieved.

IV. CONCLUSIONS

The high order elements described in this article are really suitable for electromagnetism problems since their degrees of

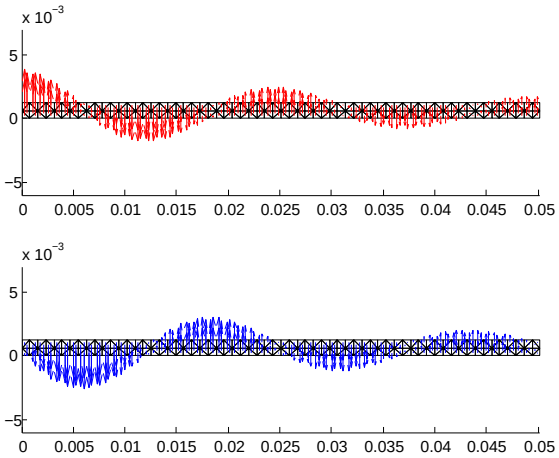

Fig. 3. Real and imaginary parts (see respectively top and bottom) of the approximated field $\mathbf{E}$ for $\sigma = 0.15$ S·m.

freedom are physical quantities related to the circulation along the small edges. The presented results show that they can be used in practice as well, indeed even with a coarse mesh we obtain a small error with respect to the exact solution and we achieve a good order of convergence.

Moreover, both the Dirichlet and the impedance boundary condition are implemented to impose the physical conditions which are typical of a waveguide problem.

A relevant feature of our implementation concerns the treatment of the linear dependence of the basis functions: indeed we didn't arbitrarily choose the redundant ones to be eliminated, but we built a new matrix to describe the relations among them in order to elegantly incorporate these constraints in the system.

This work could be a starting point for the implementation of high order edge elements in the PDE solver FreeFem++.

ACKNOWLEDGEMENT

This work was financed by the French National Research Agency (ANR) in the framework of the project MEDIMAX, ANR-13-MONU-0012.

REFERENCES

[1] J.-C. Nédélec, "Mixed finite elements in $\mathbb{R}^3$", *Numerische Mathematik*, vol. 35, pp. 315–341, 1980.

[2] F. Rapetti, "High order elements on simplicial meshes", *ESAIM*, vol. 41(6), pp 1001–1020, 2007.